Alternative Model for Mechanism-Based Inhibition of *Escherichia coli* Ribonucleotide Reductase by 2′-Azido-2′-deoxyuridine 5′-Diphosphate†

S. Salowe,‡ J. M. Bollinger, Jr., M. Ator,§ and J. Stubbe*

Departments of Chemistry and Biology, Massachusetts Institute of Technology, Cambridge, Massachusetts 02139

J. McCracken⊥ and J. Peisach

Department of Molecular Pharmacology & Physiology and Biophysics, Albert Einstein College of Medicine, Bronx, New York 10461

M. C. Samano and M. J. Robins

Department of Chemistry, Brigham Young University, Provo, Utah 84602

Received July 6, 1993; Revised Manuscript Received September 3, 1993®

ABSTRACT: Ribonucleotide reductase (RDPR) from *Escherichia coli* is composed of two subunits, R1 and R2, and catalyzes the conversion of nucleotides to deoxynucleotides. The mechanism of inactivation of RDPR by 2′-azido-2′-deoxynucleoside 5′-diphosphate (N_3UDP) has been examined using a variety of isotopically labeled derivatives: (1′-, 2′-, 3′-, or 4′-[^{2}H])-N_3UDPs and 2′-[$^{15}N_3$, ^{13}C]-N_3UDP. Electron paramagnetic resonance (EPR) and electron spin echo envelope modulation (ESEEM) spectroscopy studies using these compounds indicate that the 2′ carbon–nitrogen bond to the azide moiety is cleaved prior to or upon formation of the nitrogen-centered radical derived from the azide moiety of N_3UDP. EPR studies reveal no hyperfine interactions of the nitrogen-centered radical with the 1′, 2′, 3′, or 4′ hydrogens of N_3UDP. ESEEM studies however, reveal that the 1′ and 4′ deuterons are 3.3 ± 0.2 and 2.6 ± 0.3 Å, respectively, from the nitrogen-centered radical. Further support for carbon–nitrogen bond cleavage is derived from studies of the interaction of oxidized R1, C225SR1, and C462SR1 with R2 and N_3UDP. In all three cases, in contrast to the results with the wild type R1, azide is detected. Nitrogen-centered radical is not observed with either oxidized R1 or C225SR1 but is observed with C462SR1. These results suggest that C225 is required for the conversion of azide into N_2 and a nitrogen-centered radical. The dynamics of the inactivation of RDPR by N_3UDP have also been examined. Use of [3′-^{2}H]N_3UDP reveals an isotope effect of ~2 on the loss of the tyrosyl radical and the rate of inactivation of RDPR. In both cases the kinetics are complex, suggesting multiple modes of inactivation. In addition, several modes of inactivation are required to explain the observation that loss of the tyrosyl radical is slower than the rate of inactivation. Studies using [5′-^{3}H]N_3UDP reveal that the rapid inactivation is the result of the formation of a tight noncovalent complex between modified nucleotide, nitrogen-centered radical and RDPR. Destruction of the nitrogen-centered radical is a slow process which appears to be accompanied by decomposition of the modified nucleotide into PPi, uracil, and 2-methylene-3(2*H*)-furanone. The latter covalently modifies R1 and ultimately leads to loss of ~50% of the activity of R1.

Ribonucleotide reductases (RDPR)[1] play an essential role in DNA biosynthesis catalyzing the conversion of nucleotides to deoxynucleotides (Thelander & Reichard, 1979; Stubbe, 1989). The enzyme from *Escherichia coli* is composed of a "putative" one-to-one complex of two homodimeric subunits designated R1 and R2. R1 provides a binding site for the nucleoside diphosphate substrates (NDPs) and the allosteric effectors and contains five cysteines thought to be required for catalysis (Mao *et al.*, 1992a,b; Aberg *et al.*, 1989). R2 contains the dinuclear iron center-tyrosyl radical (Y•) essential for nucleotide reduction.

In 1976, Thelander *et al.*, reported the interesting observations that both 2′-azido-2′-deoxynucleotides and 2′-chloro-

† Supported by NIH Grants GM29595 (J.S.), American Cancer Society Grant DHP-34 (M.J.R.) and GM40168 and RR02583 (J.P.).

‡ Present address: Merck Sharp and Dohme Research Laboratories, Rahway, NJ.

§ Present address: Sterling Winthrop Pharmaceuticals Research Division, Collegeville, PA.

⊥ Present address: Department of Chemistry, Michigan State University, East Lansing, MI 48824.

® Abstract published in *Advance ACS Abstracts,* November 15, 1993.

[1] Abbreviations: RDPR, ribonucleoside diphosphate reductase; N_3UDP, 2′-azido-2′-deoxyuridine 5′-diphosphate; EPR, electron spin resonance; ESEEM, electron spin echo envelope modulation; R1, R2, the two subunits of RDPR; NDP, nucleoside 5′-diphosphate; N_3CDP, 2′-azido-2′-deoxycytidine 5′-diphosphate; Y•, tyrosyl radical; N•, nitrogen-centered radical produced on incubation of N_3UDP with RDPR; X•, a protein radical on R1 generated by long range electron transfer to the Y• on R2; HEPES, *N*-2-hydroxyethylpiperazine-*N*′-2-ethanesulfonic acid; EDTA, ethylenediamine tetraacetic acid; DTT, dithiothreitol; TRR, thioredoxin reductase; TR, thioredoxin; Urd, uridine; DMSO, dimethyl sulfoxide; DCC, dicyclohexylcarbodiimide; TLC, thin-layer chromatography; Ado, adenosine; EHNA, *erythro*-hydroxynonyladenosine; PNPase, purine nucleoside phosphorylase; UrdPase, uridine phosphorylase; N_3Urd, 2-azido-2′-deoxyuridine; N_3UMP, 2′-azido-2′-deoxyuridine 5′-monophosphate; DMF, dimethylformamide; N_3ADP, 2′-azido-2′-deoxyadenosine 5′-diphosphate; PPi, inorganic pyrophosphate; α-face, bottom face of the nucleotide; β-face, top face of the nucleotide.

0006-2960/93/0432-12749$04.00/0

Scheme I

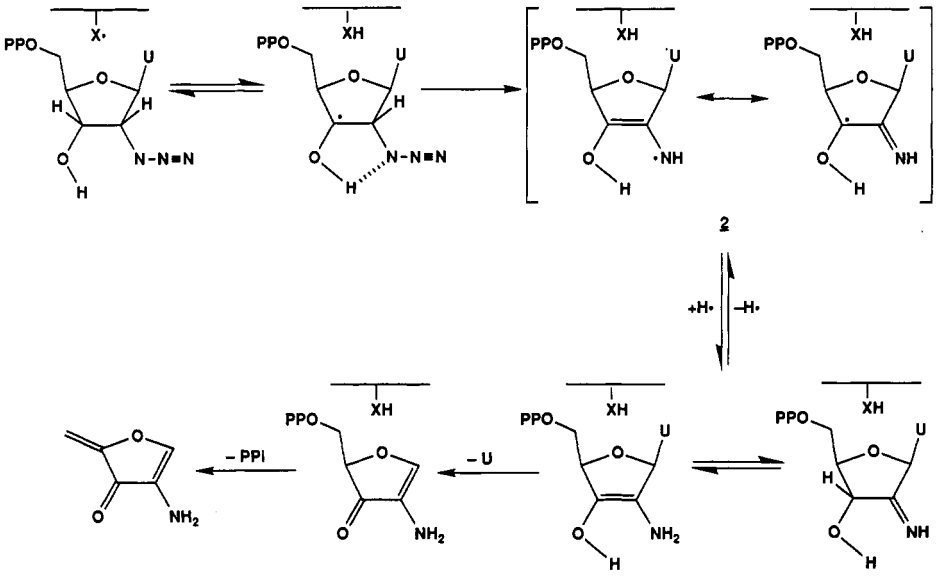

2′-deoxynucleotides are potent inactivators of *E. coli* RDPR. Studies with both of these inhibitors have provided much insight into the catalytic capabilities of this essential enzyme. In the original paper, Thelander *et al.* reported that inactivation of RDPR by 2′-azido-2′-deoxycytidine 5′-diphosphate (N_3-CDP) was accompanied by destruction of the catalytically essential Y•. In subsequent studies, Sjöberg *et al.* (1983) examined this reaction by EPR spectroscopy and reported that loss of the Y• was accompanied by transient formation of a new radical with a *g* value of 2.00 and 25 G triplet and 6.5 G doublet splittings. Isotopic labeling of the R2 subunit of RDPR with ^{15}N and ^{2}H caused no alteration of the hyperfine interactions with the new organic radical, leading to the conclusion that the new radical was derived from N_3CDP. The first conclusive evidence that the observed radical was derived from the azide moiety of the nucleotide was provided by studies using 2′-[^{15}N]N_3UDP. Incubation of this compound with RDPR produced a radical species that appeared to be identical to that reported by Sjöberg, and this isotopic substitution collapsed the observed triplet splitting into a doublet (Ator *et al.*, 1984). The observation of a substrate-derived radical provided the first direct confirmation of the ability of reductases to mediate radical generating transformations. The structure of this nitrogen-centered radical (N•), however, has remained elusive, as has the chemistry by which it is generated.

In an attempt to understand this complex reaction catalyzed by RDPR, specific isotopically labeled N_3UDPs were prepared and incubated with RDPR and the products and their stoichiometries were ascertained (Salowe *et al.*, 1987). One equivalent of N_3UDP inactivated 1 equiv of RDPR. This inactivation is accompanied by cleavage of the 3′ carbon–hydrogen bond (C–H), and production of 1 equiv each of uracil, inorganic pyrophosphate, and N_2. No N_3^- was detected. Incubation of [5′-^{3}H]N_3UDP with the protein resulted in covalent modification of R1 with 1 equiv of label, accompanied by a change in absorption of the protein at 320 nm. These results, in conjunction with the EPR studies, allowed formulation of a model (Scheme I) that accommodated all of the available information (Salowe *et al.*, 1987).

Studies in the present paper have focused on several unresolved aspects of this mechanism. First, the identity of the spin $^1/_2$ nucleus responsible for the observed 6.5 G doublet

Scheme II

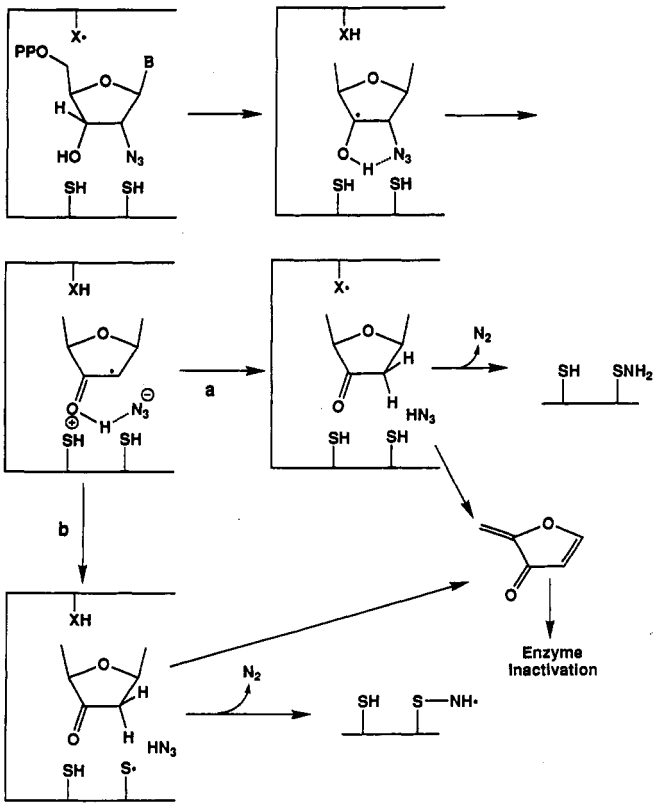

hyperfine interaction with the N• has remained a mystery but is crucial to defining the structure of the N•. Towards this end we have investigated the interaction of [1′-, 2′-, 3′-, and 4′-^{2}H]N_3UDPs and 2′-[$^{15}N_3$, ^{13}C]N_3UDP with RDPR using both electron paramagnetic resonance spectroscopy (EPR) and electron spin echo envelope modulation (ESEEM) spectroscopy. We have also investigated the interaction of modified R1s (oxidized R1 and mutated proteins C225SR1 and C462SR1) with N_3UDP. Second, we have examined the kinetics of Y• loss and enzyme inactivation using [3′-^{2}H]N_3-UDP. This new information has allowed formulation of alternative hypotheses for this complex series of transformations catalyzed by RDPR (Schemes II and III).

Scheme III

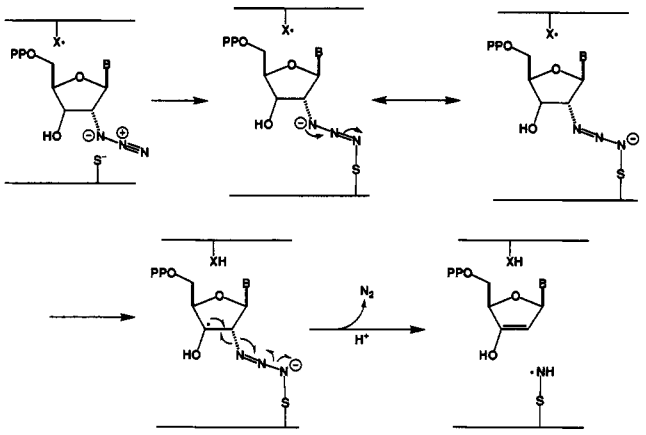

MATERIALS AND METHODS

The R2 and R1 subunits of RDPR were purified individually from overproducing *E. coli* strains N6405/pSPS2 and C600/pMB$_1$ (Salowe & Stubbe, 1986). R1 was routinely centrifuged prior to use through a 1-mL column of Sephadex G-25 (Penefsky, 1977) equilibrated in 50 mM *N*-2-hydroxyethylpiperazine-*N'*-2-ethanesulfonic acid (HEPES) pH 7.6, 15 mM magnesium sulfate, 1 mM EDTA (Buffer A) to remove dithiothreitol (DTT) in the storage buffer. Enzyme concentrations were determined from the absorbance at 280 nm using published extinction coefficients (Thelander, 1973). In the presence of 2 M guanidine-HCl the values for denatured R1 (Thelander, 1973) and apoR2 (Atkin et al., 1973) were used. Thioredoxin reductase (TRR) was isolated by modification of previously described procedures (Moore et al., 1964; Pigiet & Conley, 1977) from the overproducing *E. coli* strain SK3981 (specific activity 1000 units mg^{-1}, Lunn *et al.*, 1984). Thioredoxin (TR) was isolated from the overproducing strain K91/pMR14 (specific activity 36 units mg^{-1}; Russel and Model, 1985). C462SR1 and C225SR1 were isolated as previously described (Mao *et al.*, 1992a,b). [^{14}C]CDP was purchased from New England Nuclear.

[1'-^{2}H]Uridine (Urd). [1-^{2}H]-1-*O*-Acetyl-2,3,5-tri-*O*-benzoyl-β-D-ribofuranose (**1**) was prepared by the procedure of Kohn et al. (1965) [^{1}H NMR ($CDCl_3$) δ 7.5 (benzoyl, m), 5.90 (dd, J = 5 and 7 Hz), 5.77 (d, J = 5 Hz), 4.75 (m), 4.5 (m)]. Authentic ^{1}H material obtained from Sigma had an additional resonance at δ 6.45 (s) that was absent in the [1-^{2}H] compound. Compound **1** was converted to [1'-^{2}H]Urd by the procedure of Vorbrüggen and Bennua (1981). Following deblocking with NaOMe, the nucleoside was purified by HPLC on a semipreparative C18 reverse-phase column with H_2O as eluate (flow rate, 2.5 mL/min; retention time, 8 min): ^{1}H NMR (D_2O HOD = 4.76 ppm) δ 7.8 (C_6-H, d, $J_{5,6}$ = 8 Hz), 5.8 (C_5-H, d), 4.3 ($C_{2'}$-H, d, $J_{2',3'}$ = 5 Hz), 4.15 ($C_{3'}$-H, t, $J_{3',4'}$ = 5 Hz), 4.1 ($C_{4'}$-H, m), 3.8 ($C_{5'}$-$H_{a,b}$, AB).

[2'-^{2}H]-Urd. Urd was converted to 3',5'-di-*O*-tritylUrd and oxidized to 3',5'-di-*O*-trityl-2'-ketoUrd by the DMSO–DCC method of Cook and Moffatt (1967). The ketone was isolated by chromatography on a column of TLC grade silica gel packed in 9:1 chloroform/ethyl acetate (R_fs 2'-OH 0.05, 2'-keto 0.15) and reduced with sodium borodeuteride in ethanol as described by Cook and Moffatt (1967). The 2' epimers were detritylated in 80% acetic acid at 100 °C for 3 h. The acid was removed *in vacuo*, and the material was partitioned between water and chloroform. The aqueous layer was evaporated to yield 57% of an ~5:1 mixture of 1-(β-D-arabinofuranosyl)uracil/Urd. The epimers were separated on a 1.5 × 9 cm column of Affi-Gel 601 boronate resin (Bio-Rad) equilibrated in 0.25 M ammonium acetate, pH 8.8 in two 3-mL batches each containing approximately 13 000 A_{260} units (1.3 mmol). Samples were loaded in the high pH buffer, and the column was eluted with the same buffer until all the [2'-^{2}H]-1-(β-D-arabinofuranosyl)uracil was removed as judged by A_{260} < 0.2. [2'-^{2}H]Urd was then eluted with 0.05 M ammonium acetate pH 4.8 and desalted by reversed-phase HPLC on a C_{18} micro-bonded 10 micron, 8 mm ID radial pak cartridge (Waters). Using water as eluate at a flow rate of 2.5 mL/min, retention times were void 1.5 min, Urd 4 min: ^{1}H NMR (D_2O; HOD = 4.76 ppm) δ 7.8 (C_6-H, d, $J_{5,6}$ = 8 Hz), 5.85 ($C_{1'}$-H, s), 5.8 (C_5-H, d), 4.15 ($C_{3'}$-H, d, $J_{3',4'}$ = 5 Hz), 4.1 ($C_{4'}$-H, m), 3.8 $C_{5'}$-$H_{a,b}$, AB).

[3'-^{2}H]-Urd. This compound was prepared by a procedure analogous to that described by Stubbe and Ackles (1980) for [3'-^{3}H]Urd: ^{1}H NMR (D_2O; HOD = 4.76 ppm) δ 7.8 (C_6-H, d, $J_{5,6}$ = 8 Hz), 5.85 ($C_{1'}$-H, d, $J_{1',2'}$ = 4.5 Hz), 5.8 (C_5-H, d), 4.3 ($C_{2'}$-H, d), 4.1 ($C_{4'}$-H, t, $J_{4',5'a,b}$ = 5 Hz), 3.8 ($C_{5'}$-$H_{a,b}$, AB).

[4'-^{2}H]Urd. Preparation of [4'-^{2}H]Adenosine (Ado). The enzymatic exchange of the Ado 4' hydrogen was performed in two batches. Ado (90 mg; 337 μmol) was dissolved in 8 mL of ^2H_2O with gentle heating and then shell frozen and lyophilized. A solution of 0.1 mL each of 1 M potassium phosphate buffer pH 7.2 and 6 mM *erythro*-hydroxynonyladenosine (EHNA) was evaporated several times from ^2H_2O and finally redissolved in 2 mL of ^2H_2O. *S*-Adenosylhomocysteine hydrolase (80 μL of 6.2 mg/mL; 0.68 U/mg; a gift from Dr. R. Abeles, Brandeis University) was added, and the solution was allowed to stand for 10 min to ensure complete inhibition of contaminating adenosine deaminase. The Ado was redissolved in 8 mL of ^2H_2O and added to the solution of enzyme. The exchange was complete at 40 h as followed by the disappearance of the 4' proton signal at δ 4.15 in the NMR spectrum and the simplification of the 3' and 5' proton splittings.

A second sample of 216 mg (809 μmol) Ado was lyophilized from 18 mL of ^2H_2O and redissolved in 16 mL of ^2H_2O. A solution of 0.2 mL each of phosphate buffer and EHNA was exchanged with ^2H_2O and redissolved in 4 mL of ^2H_2O. Enzyme (300 μL) was preincubated with this solution as before, and then the Ado was added. After 13 h some precipitation was noted, so 4 mL of additional ^2H_2O was added. Exchange was complete within 46 h and the sample was frozen. The combined pool of [4'-^{2}H]Ado was boiled to denature the enzyme and then evaporated to dryness: ^{1}H NMR (D_2O; HOD = 4.65 ppm) δ 8.15 (s), 8.0 (s), 5.9 ($C_{1'}$-H, d), 4.60 (C_2-H, on side of water peak), 4.25 ($C_{3'}$-H, d), 3.70 ($C_{5'}$-$H_{a,b}$, AB).

Base Exchange Reaction. [4'-^{2}H]Ado was converted to [4'-^{2}H]Urd by the combined actions of the enzymes purine nucleoside phosphorylase (PNPase) and Urd phosphorylase (UrdPase) as described by Krenitsky et al. (1981). Uracil (50 mM) and [4'-^{2}H]Ado (5 mM) in 225 mL of 1 mM potassium phosphate, pH 7.4, 0.02% sodium azide were incubated at 37 °C with approximately 25 units PNPase and 40 units UrdPase. The progress of the reaction was monitored by reverse-phase HPLC. At a flow rate of 1.7 mL/min with water for 9 min followed by a 5-min linear gradient to 30% methanol, retention times were uracil, 3.6 min; Urd, 7.0 min; Ado, 15.3 min; and adenine, 16 min.

After equilibrium was attained (approximately 20 h), the reaction mixture was divided into three portions. Each was

diluted with an equal volume of 0.25 M ammonium acetate, pH 8.8, and adjusted to pH 8.8 by addition of 1 M ammonia. The compounds were loaded on a 1.5 × 12 cm boronate column (Affi-Gel 601; Bio-Rad) equilibrated in the same buffer and washed with more buffer until no more 260 nm absorbing material (adenine and uracil) was eluted. The nucleosides were eluted with 50 mM ammonium acetate, pH 4.8, and concentrated by evaporation under reduced pressure. Before additional portions of the reaction mixture were processed, the boronate column was washed with 0.1 M acetic acid and reequilibrated in the ammonium acetate buffer, pH 8.8.

The combined nucleosides were redissolved in 200 mL of water, adjusted to pH 10.8 with ammonia, and loaded on a 4 × 15 cm Dowex-1 (formate) column. The resin was washed with 1.5 L of water until all the Ado was eluted. Urd was then eluted with 750 mL of 0.1 M ammonium formate. The eluate was evaporated to as small a volume as possible and then desalted by repeated injections onto a semipreparative reversed-phase HPLC column in 1% methanol: yield 483 μmol [4′-^{2}H]Urd (47% based on initial [4′-^{2}H]Ado); ^{1}H NMR (D_2O, HOD = 4.76 ppm) δ 7.8 (C_6-H, d, $J_{5,6}$ = 8 Hz), 5.85 ($C_{1'}$-H, d, $J_{1',2'}$ = 4.5 Hz), 5.8 (C_5-H, d), 4.3 ($C_{2'}$-H, t, $J_{2',3'}$ = 5 Hz), 4.15 ($C_{3'}$-H, d), 3.8 ($C_{5'}$-$H_{a,b}$, AB).

2′-[$^{15}N_3$]Azido-2′-[^{13}C]deoxyuridine (2′-[$^{15}N_3$,^{13}C]N_3Urd). Treatment of D-[2-^{13}C]ribose (3 g, 20 mmol) by the procedure of Recondo and Rinderknecht (1959) gave 1-*O*-acetyl-2,3,5-tri-*O*-benzoyl-β-D-[2-^{13}C]ribofuranose (6.6 g, 65%). [2′-^{13}C]-Urd was prepared by glycosylation (Vorbrüggen & Bennua, 1981; Vorbrüggen *et al.*, 1981). To a flame-dried flask under N_2 (yields are very sensitive to H_2O) was added a solution of 2,4-bis(trimethylsilyloxy)uracil, prepared by trimethylsilylation of uracil (200 mg, 1.78 mmol), in anhydrous CH_3CN (30 mL), 1-*O*-acetyl-2,3,5-tri-*O*-benzoyl-β-D-[2-^{13}C]ribofuranose (505 mg, 1 mmol), and then trimethylsilyl trifluoromethanesulfonate (0.24 mL, 276 mg, 1.25 mmol). Stirring of the resulting clear solution was continued for 45–60 min at ambient temperature. The solution was diluted ($CHCl_3$), washed with saturated $NaHCO_3/H_2O$, and saturated NaCl/H_2O, dried (Na_2SO_4), filtered, and evaporated, and the residue was dried to give 2′,3′,5′-tri-*O*-benzoyl-[2′-^{13}C]Urd (545 mg, 98%) as a solid foam. This intermediate (535 mg, 0.96 mmol) was debenzoylated (saturated NH_3/MeOH) to give [2′-^{13}C]-Urd (220 mg, 94%, two crops from EtOH; HPLC homogeneous) which had UV and NMR spectral data identical to those of authentic Urd except for additonal spin–spin splitting: ^{1}H NMR (Me_2SO-d_6, 500 MHz) δ 4.00 ("dq", $J_{2',1'}$ = $J_{2',3'}$ = $J_{2',2'\text{-OH}}$ = 5.5 Hz, $J_{2',C2'}$ = 148 Hz, 1, H2′); ^{13}C NMR (Me_2SO-d_6, 50.28 MHz) intense signal at δ 63.78 (bs, ^{13}C2).

Treatment of [2′-^{13}C]Urd (135 mg, 0.55 mmol) according to Hampton and Nichol (1966) gave 2,2′-anhydro-1-(β-D-[2-^{13}C]arabinofuranosyl)uracil (84 mg, 67%). Treatment of this compound (70 mg, 0.31 mmol) with Li[$^{15}N_3$] (generated from Na[$^{15}N_3$] with a Dowex 50 [Li^+] column) according to Verheyden et al. (1971) and purification of the product by silica column chromatography and reversed-phase HPLC (C18; MeOH/H_2O, 1:25) gave 2′-[$^{15}N_3$]azido-2′-[^{13}C]deoxyuridine (13 mg, 15%) with chromatographic and spectral properties identical to authentic unlabeled material except for additional NMR spin–spin splitting: ^{13}C NMR (Me_2SO-d_6, 125.7 MHz) δ 64.5 (dt, $J_{C2'\text{-N}\alpha}$ = 2.6 Hz, $J_{C2'\text{-N}\beta}$ = $J_{C2'\text{-N}\gamma}$ = 1.3 Hz, ^{13}C2′); ^{15}N NMR (Me_2SO-d_6, 50.65 MHz; downfield from liquid NH_3 with external lock CH_3NO_2 set δ 380.23) δ 70.3 (bs [coupling values measured from ^{1}H, ^{13}C, and ^{15}N NMR signals], $J_{N\alpha\text{-N}\beta}$ = 14.2 Hz, $J_{N\alpha\text{-H1}'}$ = 2 Hz, $J_{N\alpha\text{-H2}'}$ = 2 Hz, $J_{N\alpha\text{-C2}'}$ = 2.6 Hz, ^{15}Nα), 208.9 (dt, $J_{N\gamma\text{-N}\beta}$ = 7.6 Hz, $J_{N\gamma\text{-N}\alpha}$ = $J_{N\gamma\text{-C2}'}$ = 0.9 Hz, ^{15}Nγ), 246.6 (dddd, $J_{N\beta\text{-C2}'}$ = 1.3 Hz, $J_{N\beta\text{-H2}'}$ = 4.3 Hz, $J_{N\beta\text{-N}\gamma}$ = 7.5 Hz, $J_{N\beta\text{-N}\alpha}$ = 14.2 Hz, ^{15}Nβ); MS (FAB) *m/z* 273 (M^+[^{13}C2′, ^{15}Nα,β,γ]), 274 (M^+[^{13}C2′, ^{15}Nα,β,γ] + 1), 113 (B + 2H).

N_3UMP. Phosphorylation of all the isotopically labeled N_3Urds was performed as previously described (Yoshikawa *et al.*, 1967). The nucleoside (100–200 μmol; dried in a vacuum dessicator) was dissolved in 0.5 mL of freshly distilled triethyl phosphate and stirred overnight at 4 °C with 2 mol equiv of freshly distilled phosphorus oxychloride. The reaction mixture was diluted into 50 mL of cold water and titrated with NaOH for approximately 1.5 h until the pH was constant at 7.0. The monophosphate was purified on a 2.5 × 21 cm column of Sephadex A-25 with a 0–0.4 M linear gradient (2 L) of triethylammonium bicarbonate (pH 7.8). The appropriate fractions eluting at 0.2 M were identified by UV absorbance, pooled, and evaporated under reduced pressure to remove triethylammonium bicarbonate. Yields were 55–60%.

An assay for phosphate (Ames & Dubin, 1960) of the N_3UMP typically revealed the presence of phosphate in excess of 1 equiv per nucleotide base. The excess phosphate was removed by the following procedure. The nucleotide (50 μmol) was dissolved in 5 mL of water in a 15-mL Cortex tube. The pH was adjusted to 8 with ammonium hydroxide, and then 1 M $BaBr_2$ (2 equiv over total phosphate) was added to precipitate inorganic phosphate. After centrifugation, the supernatant was transferred to a 30-mL Corex tube. The precipitate was rinsed with 1 mL of water and centrifuged again. This supernatant was combined with the first. The pH was adjusted to 8 again, and then five volumes of cold ethanol were added to precipitate the nucleotide. After several hours at −10 °C, the precipitate was collected by centrifugation and dried thoroughly in a vacuum dessicator. After redissolving in water, the N_3UMP was exchanged through a 1-mL column of Dowex-50 (H^+). Recovery was >90% with a final phosphate to base ratio of 1.0: ^{1}H NMR (D_2O HOD = 4.76 ppm) δ 7.8 (C_6-H, d, $J_{5,6}$ = 8 Hz), 5.8 (C_5-H, d), 5.85 ($C_{1'}$-H, d, $J_{1',2'}$ = 5 Hz), 4.25 ($C_{2'}$-H, dd, $J_{2',3'}$ = 5 Hz), 4.45 ($C_{3'}$-H, dd, $J_{3',4'}$ = 5 Hz), 4.15 ($C_{4'}$-H, m), 4.05 ($C_{5'}$-$H_{a,b}$, m).

N_3UDP. Phosphorylation of the isotopically labeled N_3-UMPs was performed by slight modification of the procedure previously described (Kozarich *et al.*, 1973). The monophosphate (58–69 μmol) was dissolved in distilled dimethylformamide (DMF), and 1 equiv of distilled tri-*n*-butylamine was added. The solvent was removed *in vacuo*, and the salt was rendered anhydrous by several evaporations from DMF. After the monophosphate was redissolved in 0.5 mL of DMF, it was mixed with 5 equiv of carbonyldiimidazole dissolved in 0.5 mL of DMF. After 3.5 h of stirring, 8 equiv of water was added (as a 1:2 solution in DMF) to destroy the excess carbonyldiimidazole. After 20 min, 5 equiv of tri-*n*-butylammonium phosphate in 0.5 mL of DMF was added and stirred for 1 day. A white precipitate formed immediately upon addition of the phosphate. The reaction mixture was diluted into 50 mL of cold water and adjusted up to pH 7.5. The diphosphate was purified on a 2.5 × 28 cm column of Sephadex A-25 using a 0–0.6 M linear gradient (2.6 L) of triethylammonium bicarbonate (pH 7.8). The appropriate UV absorbing fractions eluting at 0.35 M were pooled and evaporated under reduced pressure to remove the triethylammonium bicarbonate. Yields were 60–75%: ^{1}H NMR (D_2O HOD = 4.76 ppm) δ 7.95 (C_6-H, d, $J_{5,6}$ = 8 Hz), 5.9 (C_5-H, d), 5.95 ($C_{1'}$-H, d, $J_{1',2'}$ = 5 Hz) 4.35 ($C_{2'}$-H, dd, $J_{2',3'}$ = 5 Hz), 4.55 ($C_{3'}$-H, dd, $J_{3',4'}$ = 5 Hz), 4.15 ($C_{4'}$-H, m), 4.15 ($C_{5'}$-$H_{a,b}$, m).

N_3ADP. 2′-Azido-2′-deoxyadenosine was prepared as described (Robins *et al.*, 1992). It was phosphorylated to the diphosphate as described by Ator *et al.* (1984).

Examination of the Reaction of N_3UDP and RDPR by EPR Spectroscopy. For the experiments with the specifically deuterated N_3UDPs, the R1 and R2 subunits of RDPR were purified from *E. coli* strain KK546 (Eriksson *et al.*, 1977) as described by Ator *et al.* (1984). The enzyme was exchanged into D_2O by centrifugation through a 1-mL column of Sephadex G-25 equilibrated in buffer A (pD 7.2), in D_2O. Typical reaction mixtures contained in a final volume of 300 μL of buffer A (pD 7.2), 90 μM TTP, 0.5 mM NADPH, 180 μg of TR, 22 μg of TRR, 50–80 μM R2, and 0.4–0.7 mol equiv of R1. In experiments with N_3ADP, 0.1 mM dGTP replaced TTP as allosteric effector. For the experiment with 2′-[$^{15}N_3$, ^{13}C]N_3UDP, R1, and R2 were isolated as described by Salowe and Stubbe (1986). The reaction mixture, exchanged into D_2O as described above, contained in a final volume of 340 μL buffer A, 1.6 mM ATP, 0.5 mM NADPH, 60 μg of TRR, 36 μg of TR, and 79 μM RDPR (1:1 subunit ratio).

Samples were transferred to 48-mm (diameter) quartz tubes and rapidly frozen by dipping in liquid nitrogen or in liquid nitrogen cooled isopentane. X-band spectra at 13 K were obtained in the laboratory of Professor Helmut Beinert (University of Wisconsin, Madison) on a Varian E-109 spectrometer equipped with a 9-in. magnet, E-102 microwave bridge, and an E-900 acquisition system. Spectra at 77 K were obtained in the laboratory of Professor George Reed on the same instrument or on a standard Varian E-109 spectrometer system at the National Biomedical ESR Center, Medical College of Wisconsin. More recently spectra were obtained at 100 K on a Brüker Model ESP 300 spectrometer maintained at constant temperature with a Brüker ER4111VT variable temperature controller. After recording the spectrum of the Y•, the sample was thawed by rapid immersion into a water bath at room temperature and equilibrated at 25 °C. N_3UDP was then added to a final concentration of 1 or 0.48 mM in the case of 2′-[$^{15}N_3$, ^{13}C]N_3UDP to start the reaction. In the study with N_3ADP, the nucleotide was added to a final concentration of 0.5 mM. After an appropriate incubation time (4–7 min) the sample was refrozen in liquid nitrogen, and the spectrum was recorded. Subsequent timepoints were taken after thawing, incubating, and refreezing in a like manner.

Examination of the Reaction of N_3UDP and RDPR by ESEEM Spectroscopy. The subunits of RDPR were isolated as described by Salowe and Stubbe (1986). The proteins were centrifuged through a 1-mL column of Sephadex G-25 equilibrated in buffer A. Samples contained in a final volume of 150 μL: buffer A, 0.1 mM TTP, 0.5 mM NADPH, 2 μg of TRR, 7 μg of TR, and 90 μM RDPR (1:1 subunit ratio). After freezing in liquid nitrogen as described above, the initial Y• spectrum was recorded. The sample was then thawed and equilibrated at 25 °C. N_3UDP (deuterated or unlabeled) was added to a final concentration of 0.5 mM. After 5 min, the sample was refrozen in liquid nitrogen.

ESEEM spectra were obtained at the Albert Einstein College of Medicine. The instrument design has been described elsewhere (McCracken *et al.*, 1987) and uses a cavity described by Britt and Klein (1987). Spectra were recorded at 1.8 or 4.2 K with a microwave frequency of 9.07 GHz and magnetic field of 3200 G. Both two pulse and three pulse or stimulated echo sequences (Mims & Peisach, 1989) were used. The microwave pulse power was approximately 50 W for the two pulse and 30 W for the three pulse sequences. Data collection was controlled by an Apple II-plus computer.

Interaction of N_3UDP with C225SR1. The rate of Y• loss and formation of azide ion were determined by the following procedures. DTT was removed from R1 by the procedure of Penefsky (1977). The assay mixture contained in a final volume of 345 μL: 15 μM C225SR1, 16 μM R2, 79 μM NADPH, 1.6 mM ATP, 5.4 μg of TRR, 10 μg of TR, 470 μM N_3UDP, and buffer A. All components except R2 and N_3UDP were mixed and placed in a cuvette, and an absorption spectrum was recorded from 300–480 nm. R2 was added, and a spectrum was again acquired. Finally the N_3UDP was added, and the reaction was monitored spectrophotometrically every 5 s for 25 min. Aliquots from the reaction were removed, and the reaction was quenched by incubation in a boiling water bath for 2 min. The quenched reaction mixture was centrifuged to pellet the denatured protein. A control was performed in which only N_3UDP in buffer was incubated in a boiling water bath for 2 min. Azide ion was quantified by two different procedures as described (Salowe *et al.*, 1987). Analysis for the N• was carried out as follows: R1 and R2 were run through a Sephadex G-50 column in D_2O and buffer A. The reaction mixture in D_2O contained 38 μM C225SR1, 38 μM R2, 1 mM NADPH, 33 μg of TR, 9 μg of TRR, 1.6 mM ATP, 580 μM N_3UDP. The reaction was incubated at 27 °C for 8 min and frozen in an EPR tube. The contents of the reaction mixture were thawed and incubated at 25 °C for various time periods over 4 h and then periodically refrozen and the EPR spectrum recorded. The control experiments contained metR2 (R2 in which the Y• has been reduced by hydroxyurea) in place of R2.

Isotope Effect upon Inactivation of RDPR by [3′-^{2}H]N_3-UDP. Each timepoint for the inactivation progress curve contained in a final volume of 100 μL: buffer A, 0.1 mM TTP, 0.25 mM NADPH, 0.2 μg of TRR, 0.8 μg of TR, and 1 μM RDPR (1:1 subunit ratio). The reaction was initiated by the addition of 10 μL of a stock solution of N_3UDP or [3′-^{2}H]N_3UDP. After 10–120 s, 100 μL was withdrawn and diluted into a cuvette containing 900 μL of assay solution composed of buffer A, 1.6 mM ATP, 0.25 mM NADPH, 2.0 mM CDP, 2.7 μg of TRR, and 10.8 μg of TR. The steady-state decrease in absorbance at 340 nm was recorded after a lag of several minutes duration. This lag was not evident at the initial time point prior to the addition of N_3UDP and was thus not a result of the coupled assay. Both the inactivation reaction and subsequent assay were conducted at 25 °C.

Isotope Effect upon Y• Loss, [3′-^{2}H]N_3UDP with RDPR. A cuvette containing buffer A, 0.1 mM TTP, 0.25 mM NADPH, 3 μg of TRR, 9 μg of TR, and 10 μM RDPR in a volume of 800 μL was placed in the spectrophotometer sample compartment thermostated at 25 °C. A reference cuvette contained only the buffer and nucleotide components. The reaction was initiated by the addition of 10 μL of N_3UDP or [3′-^{2}H]-N_3UDP to a final concentration of 55 μM. After mixing (dead time 10–15 s) the absorbance at 410 nm was recorded continuously for 15 min. The endpoint for radical loss was then established by adding 10 μL of 1 M hydroxyurea and incubating for an additional 30 min.

R1 Inactivation Time Course. The reaction mixture contained buffer A, 0.1 mM TTP, 0.5 mM NADPH, 3.6 μg/mL of TRR, 14.4 μg/mL of TR, an 10 μM RDPR. A 5-μL aliquot was removed for the determination of initial activity, and then N_3UDP was added to the reaction to a final concentration of 150 μM. Additional 5-μL aliquots were removed at various timepoints for dilution into 95 μL of an

assay mixture containing buffer A, 1.6 mM ATP, 1 mM NADPH, 1.5 mM [^{14}C]CDP (specific activity 7.6×10^5 cpm/μmol), 2.5 μg of TR, 10 μg of TR, and 10 μM R2. After 5 min at 25 °C, the assay was terminated by a 1-min incubation in a boiling water bath and worked up as previously described (Salowe *et al.*, 1987).

Radiolabeling of RDPR with [5′-^{3}H]N_3UDP. Three parallel reactions were prepared each containing buffer A, 0.25 mM TTP, 0.5 mM NADPH, 1 μg of TRR, 4 μg of TR, and 55 μM RDPR (1:1 subunit ratio) in 100 μL. Each reaction was initiated by the addition of [5′-^{3}H]N_3UDP to a final concentration of 215 μM. Enzymatic activity was measured prior to the addition of the inhibitor and at various times subsequent to its addition. A 5-μL aliquot of the reaction mixture was diluted 15-fold into buffer A, and then 10 μL of this diluted solution was withdrawn for an assay using [^{14}C]CDP (Salowe *et al.*, 1987). After a 10-min incubation with N_3UDP, one of the three reactions was diluted with 300 μL of cold 50 mM HEPES buffer (pH 7.6) and passed through a 1.5 × 15 cm Sephadex G-50 column in the same buffer. A second reaction was also incubated for 10 min but was diluted with 300 μL of 8 M guanidine-HCl and 67 mM DTT prepared in 50 mM HEPES, pH 7.6. After 15 min at room temperature, the protein was passed through a Sephadex G-50 column equilibrated in 50 mM HEPES, pH 7.6, containing 2 M guanidine–HCl. The third reaction was treated identically to the second after a 90-min incubation. Protein-containing fractions were identified by A_{280} and pooled. The amount of bound radioactivity was determined by scintillation counting of an aliquot of the protein.

Incubation of Oxidized R1 with N_3UDP. R1 (60 μM) and R2 (55 μM) were incubated in buffer A with 1.5 mM ATP and 0.5 mM CDP for 4 min at 25 °C. The oxidized R1 was then separated from the small molecules by the procedure of Penefsky (1977). The preoxidized R1 R2 was then incubated with N_3UDP (510 μM) and 1.6 mM ATP at 25 °C. While the reaction was monitored spectrophometrically, six 30-μL aliquots were withdrawn at various times (from 2.5 to 90 min) and quenched by incubation for 2 min in a boiling H_2O bath. Each of these time points were analyzed for azide ion (Salowe *et al.*, 1987). The remaining solution was adjusted to pH 8.5 with 0.5 M Tris-HCl, treated at 37 °C for 3 h with 2 units of alkaline phosphatase, and analyzed for uracil by HPLC. The retention time for uracil is 6 min on a ODS-II reverse-phase HPLC column eluted with a flow rate of 1 mL/min.

RESULTS

EPR Spectroscopy of 2′-[$^{15}N_3$,^{13}C]N_3UDP with RDPR: Attempts To Characterize the N•. Previous studies demonstrated that incubation of N_3NDP with RDPR resulted in loss of the Y• of the R2 subunit concomitant with formation of a N• and N_2. Isotopic labeling studies with [^{15}N]-N_3UDP established that the N• is derived from the azide moiety of the nucleotide and has hyperfine interaction with an $I = {}^1/_2$ nucleus of unknown identity. Based on the EPR data and extensive analysis of the reaction products, the structure of the N• was previously proposed to be **2** (Scheme I) (Salowe *et al.*, 1987). To test the validity of this proposal and to identify the source of the $I = {}^1/_2$ nucleus giving rise to a 6.5 G hyperfine interaction, 2′-[$^{15}N_3$,^{13}C]N_3UDP and [1′-^{2}H]-, [3′-^{2}H]-, and [4′-^{2}H]N_3UDPs were prepared and incubated with the enzyme. All of these compounds, except 2′-[$^{15}N_3$,^{13}C]N_3-UDP, resulted in the production of an EPR spectrum virtually identical to that observed with a control using unlabeled N_3-UDP (Figure 1). The spectra in all cases are a superposition of the N• and the Y• of R2. Spectra resulting from generation of N• from 2′-[$^{15}N_3$,^{13}C]N_3UDP and 2′-[$^{15}N_3$,^{12}C]N_3UDP are shown in Figure 2 (parts A and B, respectively). Several conclusions can be drawn from these experiments. First, the lack of an observable hyperfine interaction between the [^{15}N]-N• and ^{13}C ($I = {}^1/_2$) of 2′-[$^{15}N_3$,^{13}C]N_3UDP suggests that the 2′-[^{13}C–^{15}N] bond originally present in the N_3UDP has been cleaved. This result is in contrast to that predicted for intermediate **2** in Scheme I (Salowe *et al.*, 1987) and demands an alternative model. Second, the observations that successive deuterium substitution of the hydrogens at C-1′, C-3′, C-4′, and previously at C-2′, of N_3UDP had no effect on the observed hyperfine interaction of 6.5 G, suggest that the coupling is not derived from a nucleus attached to the nucleotide.[2] Previous failures to alter this hyperfine interaction when the reaction was carried out in D_2O and when the totally ^{2}H labeled R2 subunit was employed (Sjöberg *et al.*, 1983; Ator *et al.*, 1987) in conjunction with studies reported herein, suggest that the hyperfine interaction must arise from interaction of N• with an $I = {}^1/_2$ nucleus from the R1 subunit.

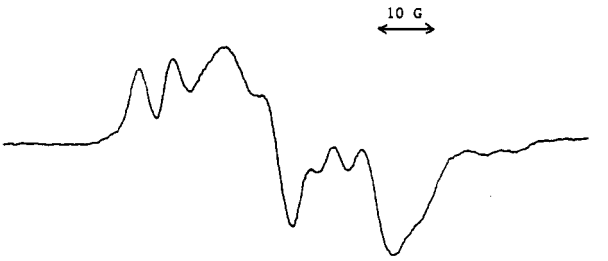

FIGURE 1: EPR spectrum obtained four min after addition of [4′-^{2}H]N_3UDP to RDPR. Spectrometer conditions: microwave frequency, 9.07 GHz; microwave power, 1 mW; modulation amplitude, 2 G; temperature, 77 K; scanning rate, 50 G/min; time constant, 0.128 s. Similar results were obtained with [1′ and 3′-^{2}H]N_3UDPs.

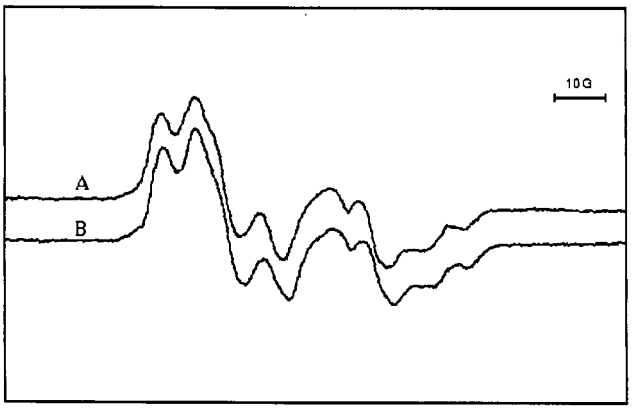

FIGURE 2: EPR spectrum obtained 6 min after addition of either [2′-^{13}C,^{15}N]N_3UDP (top) or [2′-^{12}C,^{15}N]N_3UDP (bottom) to RDPR. The spectra are superimposable ±1 G. Spectrometer conditions: microwave frequency, 9.41 GHz; microwave power 10 μW; modulation amplitude, 1 G; temperature 40 K; scan time 2.8 G/min; time constant 0.128 s.

ESEEM Studies Using Specifically Labeled 1′-, 2′-, 3′-, or 4′-[^{2}H]N_3UDPs: Probes of the Structure of N•. The structure of the transient N• was further investigated using ESEEM spectroscopy. This technique allows the detection of dipolar interactions of an electron spin, such as the N•, with neighboring deuteriated nuclei, such as 1′-, 2′-, 3′-, or 4′-[^{2}H]N_3UDPs that are within 6 Å of one another (Peisach *et*

[2] The fact that both N_3UDP and N_3ADP give rise to an identical EPR signal suggests that the hyperfine interaction is not derived from the base.

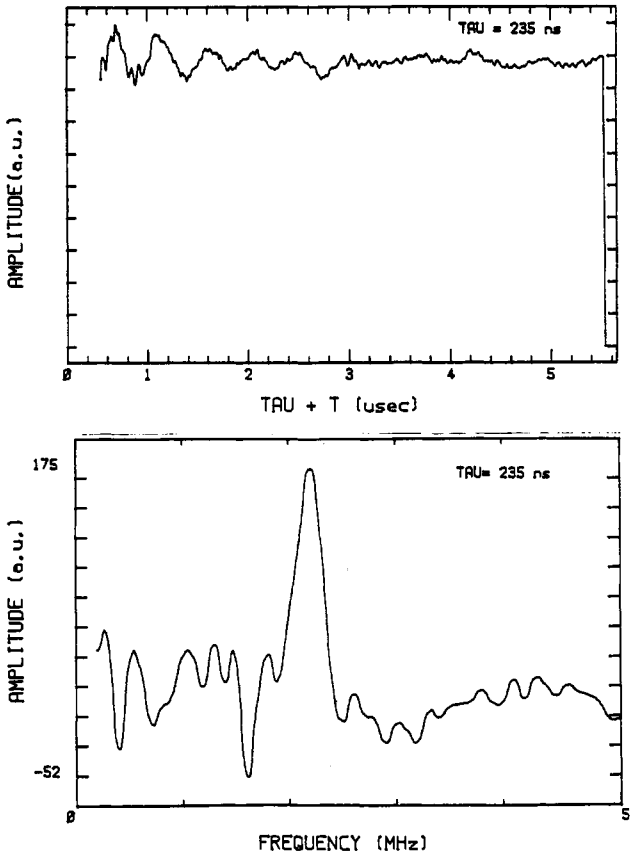

FIGURE 3: ESEEM spectra obtained during the reaction of [1′-^{2}H]N_3UDP with RDPR. (A) Time domain spectrum from a three pulse stimulated echo sequence. ^{1}H frequencies have been ratioed out. (B) Frequency domain spectrum obtained from Fourier transformation of the spectrum in (A).

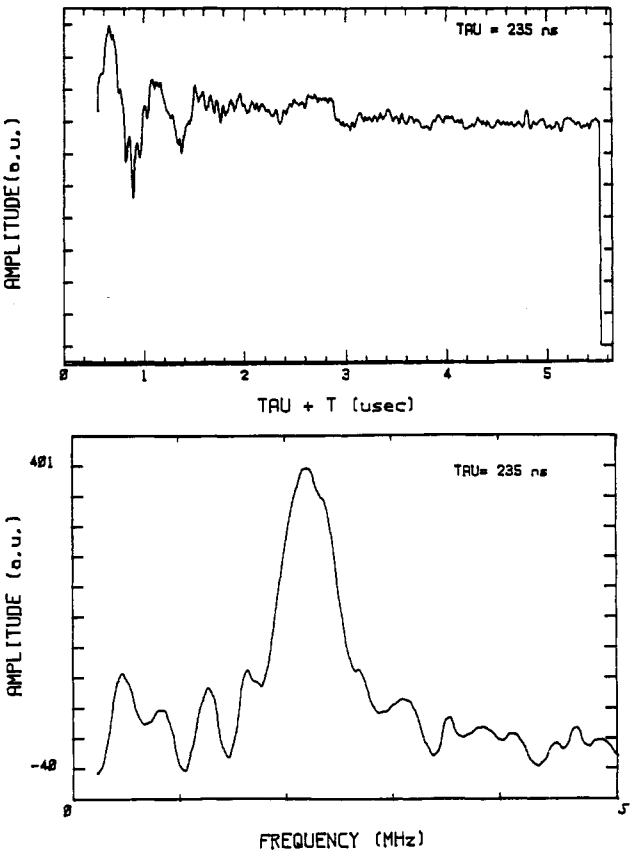

FIGURE 4: ESEEM spectra obtained during the reaction of [4′-^{2}H]N_3UDP with RDPR. (A) Time domain spectrum from a three pulse stimulated echo sequence. ^{1}H frequencies have been ratioed out. (B) Frequency domain spectrum obtained from Fourier transformation of the spectrum in (A).

al., 1979). The method involves application of intense microwave pulses and recording of the echo decay envelope (Mims & Peisach, 1989). The periodic modulations in the decay are attributable to coupling between the electron spin and the nearby nuclear spins. The depth and the frequency of these modulations convey information about the identity, number, and distance of nearby nuclei to the electron. The labeled and control (unlabeled) N_3UDPs were incubated for 5 min with RDPR and the echo envelope of each was recorded. While no deuterium modulations were observed with the unlabeled N_3UDP control, Figures 3 and 4 show that deuterium modulations are apparent in the reactions of RDPR with both [1′-^{2}H]N_3UDP and [4′-^{2}H]N_3UDP. Two sets of data were collected for each sample. In both cases the deuterium modulation depth was ~2-fold deeper for the [4′-^{2}H]N_3N_3UDP than for the [1′-^{2}H]N_3UDP.

In an effort to quantitate the results in terms of differences in dipolar distances between the deuterons and the radical, ESEEM spectral simulations using the approach described by Magliozzo *et al.* (1987) were undertaken. For comparison with computer simulations the data sets need to be corrected for background decay and interferences from Y• contamination. Reactions with unprotonated N_3UDP were used as controls. The spectra shown in Figures 3 and 4 were obtained by "ratioing" the experimental data with the control data in order to isolate the ESEEM due only to coupled deuterons (Mims *et al.*, 1984). Because both deuterated N_3UDP and control data sets showed shallow modulations, errors that arise from cross terms generated by this procedure are expected to be small. The results show that for the [4′-^{2}H]N_3UDP, the deuterium envelope modulation depths were 35% (±10%) of the average echo amplitude, while with the [1′-^{2}H]N_3UDP, the deuterium envelope modulation depths were about 15% (±5%). Analysis of these results indicates that for [4′-^{2}H]N_3-UDP, the deuteron has a dipole–dipole distance from the paramagnetic species (presumably the N•) of 2.6 ± 0.3 Å, and for [1′-^{2}H]N_3UDP, a distance of 3.3 ± 0.2 Å.

Since the X band EPR spectrum of each sample reveals that the amount of Y• remaining in each sample is about the same, we can confidently conclude that the deuteron from the 4′-position is closer than the deuteron from the 1′-position to the paramagnetic species. Since the substrate binds to the R1 subunit and the tyrosyl radical is buried 10 Å from the surface of the R2 subunit (Nordlund *et al.*, 1990), it is reasonable to conclude that the N• (rather than the Y•) is experiencing magnetic interactions with the 1′- and 4′-^{2}Hs of the sugar moiety of the isotopically labeled nucleotide. Furthermore, since the N• is formed at the expense of Y•, it is reasonable to conclude that no molecule contains both a Y• and a N•. Finally, no deuterium modulations were observed with either [2′-^{2}H] or [3′-^{2}H]N_3UDPs. These results indicate that, even though the original 2′ C–N bond has been cleaved, releasing a species that is ultimately converted to the N•, the 1′ and 4′ hydrogens on the α face (bottom face) of the modified sugar ring are close within three-dimensional space to N•. The 3′ and 2′ hydrogens originally on the β-face (top face) of the modified sugar are believed to be >6 Å removed from the N•.

Further Evidence for 2′ C–N Bond Cleavage. The studies with 2′-[$^{15}N_3$,^{13}C]N_3UDP suggest that the 2′ C–N bond of the azido-nucleotide is cleaved prior to or during formation of the N•. In the former case either N_3^- or N_3• might be the

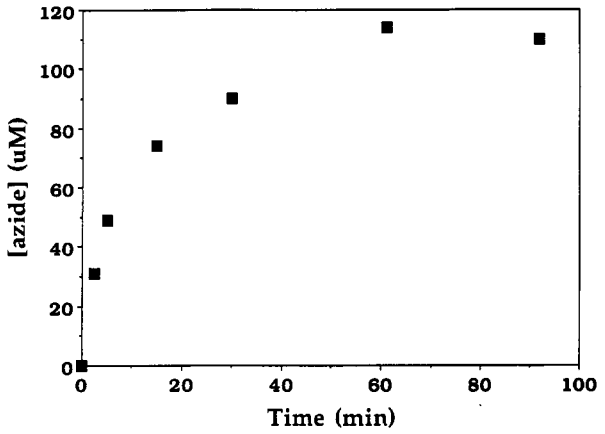

FIGURE 5: Time-dependent formation of azide ion resulting from incubation of N_3UDP with oxidized R1 and R2.

expected precursor of N_2 and N•. As indicated in eq 1, a chemical model system provides precedent for this type of transformation involving "azide" loss. Treatment of **3** with Bu_3SnH resulted in production of **5** (and not the anticipated **4**) in 65% yield (Madhavan & Martin, 1985). Although the mechanism of this reaction was not investigated, a reasonable model suggests that, subsequent to generation of a radical β to the alkyl azide, either N_3^- or N_3• is lost.

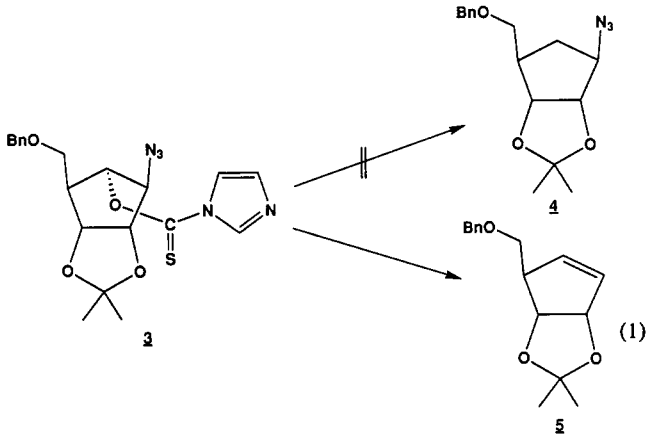

Previous studies of Salowe *et al.* (1987) indicated that oxidized RDPR, prepared by incubation of reduced RDPR with CDP in the absence of an external reductant, appeared not to be inactivated upon incubation with N_3UDP, nor was the Y• lost. Based on these observations, it was concluded that the reduced thiols were required for the enzyme catalyzed destruction of N_3UDP. In these experiments, however, no analysis for azide was performed. Given the EPR results (Figure 2) and the model studies (eq 1), we repeated this experiment and analyzed for azide ion. Preoxidized RDPR (25 μM) was incubated with N_3UDP and ATP in the absence of any external reductant. The reaction mixture was monitored for Y• loss, uracil production, and N_3^- release as a function of time (although azide ion is detected by our assay methods, since N_3• is rapidly reduced to N_3^-, a distinction between these two options cannot be made). As previously reported <10% loss of the Y• of R2 occurs over 60 min. However, N_3^- (Figure 5) and uracil are produced in a time dependent fashion, and this process appears to be accompanied by a very slow inactivation and a change in absorbance at 320 nm on the protein. At the 60 min time point, 4.3 mol of N_3^-/R1 and 4.3 mol of uracil/R_1 are detected. These results support the thesis that the 2′ C–N bond is cleaved and suggest that the redox active thiols within the active site play a key role in the conversion of some form of azide to N_2 and the N•.

Interaction of N_3UDP with C225SR1 and C462R1. Recent site-directed mutagenesis studies have suggested that C225 and C462 are the cysteines directly involved in nucleotide reduction (Mao *et al.*, 1989, 1992a,b). To provide further support for RDPR mediated 2′ C–N cleavage and to address the possible role of these cysteines in formation of N_2 and N•, the interaction of each of these R1 mutants with N_3UDP was investigated.

N_3UDP was incubated with C225SR1/R2 and ATP, and the reaction was monitored for loss of Y•, formation of N•, formation of azide ion, and change in the absorbance at 320 nm. Incubation of 5 nmol of RDPR with N_3UDP resulted in the production of 15 nmol of azide ion. Azide release was accompanied by a change in absorption at 320 nm on the protein. Efforts to detect formation of N• using EPR spectroscopy failed to reveal any signal other than that of the Y• on R2. These results substantiate the conclusion that RDPR catalyzes 2′ C–N bond cleavage and suggest that C225 plays a key role in the conversion of the azide moiety to N_2 and N•.

Similar preliminary experiments with C462SR1 indicate that uracil (1–2 mol/mol R1) is released, along with a small amount of azide ion (0.1–0.15 mol/mol R1). As in the case of both oxidized R1 and C225SR1, the chemistry is accompanied by a change in absorbance at 320 nm on the protein. EPR analysis of the products revealed that N• is produced by R1C462S and that Y• is also lost. These data again support the conclusion that the RDPR catalyzes the release of an azide moiety and that C462 is not required for N• production.

Kinetics of the Interaction of [3′-^{2}H]-N_3UDP with RDPR. Previous studies have shown that inactivation of RDPR by N_3UDP is accompanied by Y• destruction within the R2 subunit and 3′ C–H bond cleavage of the nucleotide. Our model for the mechanism of nucleotide reduction suggests that the Y• or a protein radical in equilibrium with this radical (X• in Schemes I–III) abstracts the 3′ hydrogen to initiate catalysis (Stubbe, 1990; Mao *et al.*, 1992a,b). Since both cleavage of the 3′ C–H bond of substrate and reduction of the protein radical occur, this model can be tested directly. [3′-^{2}H]-N_3UDP was prepared, and the rate of loss of Y• as a function of time was monitored by decrease in absorbance at 410 nm. As demonstrated in Figure 6 using a 1:1 mixture of R1 and R2, an isotope effect on loss of the Y• is observed. The kinetics, however, are multiphasic, and no apparent isotope effect is observed during the slow, second phase of the reaction.

Nature of Enzyme Inactivation. Evidence for a Tight Noncovalent Complex Preceding Covalent Modification. As expected from the isotope effect studies described above, the rate of inactivation of RDPR is also isotope sensitive. Figure 7 compares inactivation progress curves for N_3UDP and [3′-^{2}H]N_3UDP at several concentrations. The deuterated compound inactivates RDPR more slowly than the unlabeled compound at concentrations of 13, 50, and 200 μM. Similar results were obtained at intermediate concentrations of 25 and 100 μM (data not shown). As in the case of monitoring Y• loss at 410 nm (Figure 6), the semilog plots are curved at all concentrations, and therefore no meaningful rate constants can be extracted from the data. Comparison of the curves shows that 50% inactivation requires about twice as long with [3′-^{2}H]N_3UDP as with unlabeled N_3UDP. No isotope effect upon inactivation is observed with [2′-^{2}H]-N_3UDP at 25 μM (data not shown).

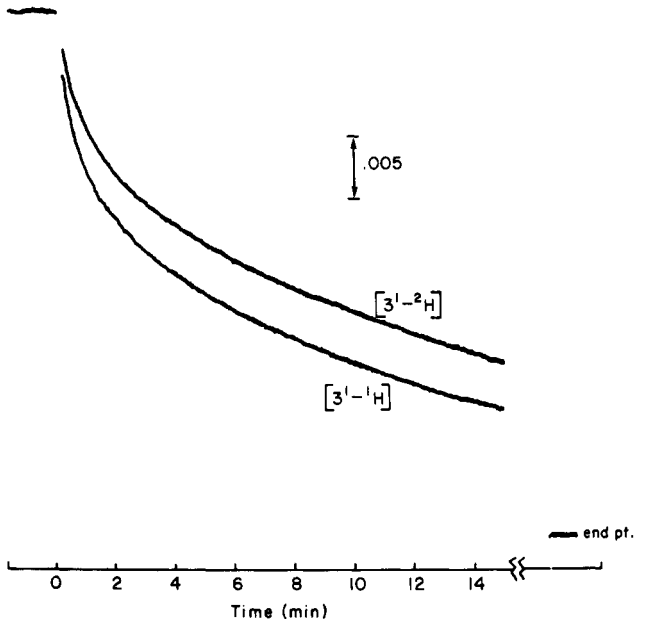

FIGURE 6: Isotope effect on Y• loss. The reaction of RDPR with 55 μM N_3UDP or [3'-^{2}H]N_3UDP was initiated and monitored for loss of Y• absorbance at 410 nm.

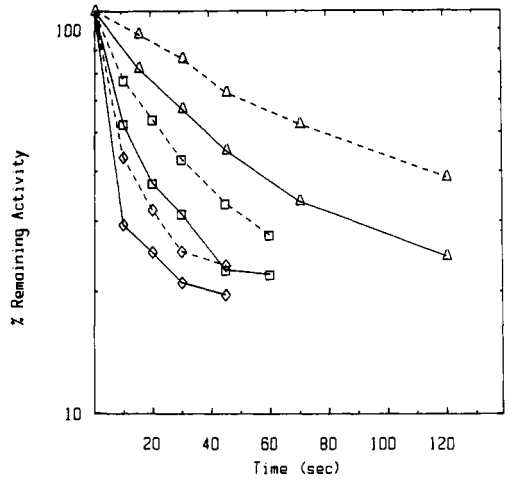

FIGURE 7: Isotope effect on the inactivation of RDPR by N_3UDP (—) and [3'-^{2}H]N_3UDP (– –): results are shown for inactivator concentrations of 12.6 (△), 50 (□), and 200 μM (◇). Data for 25 and 100 μM are omitted for clarity.

To determine whether covalent modification occurs on the same time scale as enzyme inactivation, RDPR was incubated with [5'-^{3}H]N_3UDP for a short time and then reisolated by gel filtration under denaturing and nondenaturing conditions. After 10 min, the enzyme was 72% inactivated and had 0.66 mol ^{3}H bound per mol enzyme when reisolated in the native state. When denatured with 6 M guanidine–HCl after the 10 min incubation, only 0.14 mol ^{3}H remained bound per mol enzyme. The radioactivity associated with the protein, therefore, appears to be noncovalently (or reversibly covalently) bound. In contrast, after extended incubation (90 min), denaturing with guanidine–HCl did not release the radioactivity, and 0.81 mol ^{3}H label were bound per mol RDPR. Thus, irreversible modification of the protein occurs on a slower time scale than initial radiolabeling and inactivation.

Time Course of R1 Inactivation. We have previously reported that the R1 subunit of RDPR is covalently modified and partially inactivated by reaction with N_3UDP (Salowe *et al.*, 1987). A time course of R1 inactivation is shown in Figure 8. Surprisingly, R1 activity rapidly decreases during the first 10 min to a minimum below 50% before slowly recovering a final value of approximately 50% of starting R1 activity. In several repetitions of this experiment, the minimum R1 activity achieved has ranged from 20 to 40% of the initial activity, while the endpoint after extended incubation has ranged from 40 to 60%. The data in Figure 8 were fit to an equation describing two consecutive first-order reactions:

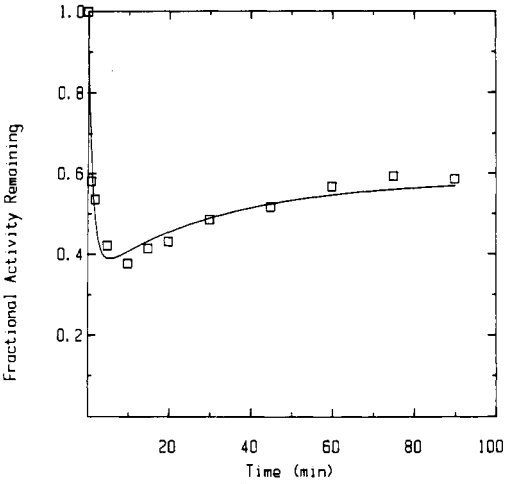

FIGURE 8: Time-dependent inactivation of R1. RDPR (10 μM) was incubated with 150 μM N_3UDP, and aliquots were removed at various times for the determination of residual R1 activity. The solid line is calculated as described in the text.

$$R1 \xrightarrow{k_1} R1^0 \xrightarrow{k_2} R1^*$$

$$Y = A + Be^{-k_1 t} + Ce^{-k_2 t}$$

$R1^0$ represents a completely inactive form of the subunit, R1* represents a modified form with approximately one-half the original specific activity, and k_1 and k_2 are rate constants. Y is the fraction of remaining activity, t is time, and A, B, and C are constants. For fitting the data in Figure 8, A was set equal to 0.585 , the apparent final value of recovered R1 activity in this experiment. After least-squares fitting, values obtained for the rate constants were k_1 = 0.81 min^{-1} ($t_{1/2}$ = 0.86 min) and k_2 = 0.03 min^{-1} ($t_{1/2}$ = 23 min).

DISCUSSION

2'-Azido-2'-deoxynucleotides are "stoichiometric" mechanism-based inhibitors of *E. coli* RDPR (Thelander *et al.*, 1976; Salowe *et al.*, 1987). Incubation of isotopically labeled N_3UDPs with enzyme has allowed isolation, identification, and quantitation of the following products: PP_i, uracil, and N_2. This process is initiated by 3' C–H bond cleavage, demonstrated as ^3H_2O release from [3'-^{3}H]N_3UDP, and is accompanied by "stoichiometric" reduction of the Y• on R2 and "stoichiometric" covalent modification of R1. This covalent labeling is accompanied by an increase in the protein absorption at 320 nm, consistent with alkylation by 2-methylene-3(2*H*)-furanone (Stubbe, 1989). The model originally proposed to accommodate this information is shown in Scheme I (Salowe *et al.*, 1987). Labeling studies with [1'-, 2'-, 3'-, or 4'-^{2}H]N_3UDPs and 2'-[$^{15}N_3$,^{13}C]N_3UDP, studies with oxidized R1 and with site-directed mutants of R1 (C225S and C462S), and kinetic analysis of this process, however, have required modification of this model (see Schemes II and III).

The model in Scheme I predicted that the N• is covalently attached to the C-2' carbon of the ribose moiety of N_3UDP.

Two sets of experiments now suggest that this bond is cleaved prior to, or possibly concomitant with (Scheme III), formation of the N•. (1) No additional hyperfine interaction is apparent in the EPR spectrum of N• generated by incubation of 2′-[$^{15}N_3$,^{13}C]N_3UDP with RDPR. Although no appropriate model systems to define the strength of such an interaction have been identified, the spectrum from the 2′-[$^{15}N_3$,^{13}C]N_3-UDP experiment is virtually superimposable on that recorded for the control ^{12}C-labeled compound. (2) Studies of N_3-UDP with oxidized RDPR or mutants, C225SR1R2 or C462SR1R2, indicate that some form of azide (N_3^-, N_3•, HN_3) is released during the incubation. The method of assay, coordination of N_3^- to the heme of ferric hemoglobin, cannot distinguish between these possibilities, since both N_3• and HN_3 would be converted rapidly to N_3^-. In the case of C225SR1, no N• is detected and, therefore, presumably no N_2 is produced. In the case of oxidized R1, no Y• is lost, and again presumably no N• is produced. However, with C462SR1, N• is detected and Y• of R2 is lost. These data can be interpreted to indicate that C225 plays an essential role in the conversion of some form of azide into N_2 and N•. This is consistent with the proposed role of this cysteine in the normal reduction process (Mao *et al.*, 1992a,b). The normal reduction process occurs with retention of configuration and thus requires that the reducing equivalents are delivered from the α face of the nucleotide. Likewise, the azido moiety is located on the α face of N_3UDP, and, thus, it is reasonable that the observed chemistry would also occur from this face.

These data suggest several alternative models indicated in Schemes II and III. The model in Scheme II differs from that originally proposed (Scheme I) in that subsequent to 3′ hydrogen atom abstraction some form of azide is lost. Following reduction by electron and proton transfer or by hydrogen atom transfer, a 3′-ketodeoxyuridine 5′-diphosphate is generated. This 3′-ketonucleotide might dissociate from the active site upon quenching of the N• radical. Its decomposition would produce PP_i, uracil and 2-methylene-3(2*H*)-furanone. Alkylation of the protein by the furanone would result in the change in absorbance at 320 nm. Reaction of the released azide with a cysteinate or cysteinyl radical could result in formation of N_2 and N•.

A second model to accommodate the observed results is shown in Scheme III. Previous studies (Cartwright *et al.*, 1976; Stavos *et al.*, 1978) have indicated that aryl and alkyl azides can be reduced by DTT to produce aryl (alkyl) amines and oxidized DTT. Several mechanisms have been proposed to account for these products, one involving nucleophilic attack of a thiolate on the terminal nitrogen of the azide. The first step of the reaction of N_3UDP with RDPR, based on this model, could be envisioned to involve, therefore, nucleophilic attack of the C225 thiolate on the terminal nitrogen of the azide moiety of the 2′-azidonucleotide (or nucleotide radical). In contrast to the model systems, however, we know that no 2′-amino-2′-deoxynucleotide is produced (unpublished results) and that C462 is not required for this process and therefore that no disulfide between C462 and C225 is formed. We therefore propose that this intermediate decomposes as shown, to produce N• and the 3′-ketonucleotide. To our knowledge this step is chemically unprecedented. The most unappealing aspect of this proposed mechanism is that a different mechanism, namely loss of N_3^- and formation of a cation radical intermediate, is required to accommodate the results with the oxidized and mutant R1s. These considerations persuade us to favor the reaction sequence shown in Scheme II.

Key unresolved questions are the structure of the N• and an explanation for its amazing stability. The EPR spectrum of the N• was interpreted to indicate that the unpaired electron is predominantly localized on a single nitrogen derived from the azide moiety of N_3UDP and interacts directly with a proton (Sjoberg *et al.*, 1983; Ator *et al.*, 1984). However, ^2H labeling at the 1′, 2′, 3′, or 4′ positions of N_3UDP fail to alter the spectrum [Figure 1 and Ator *et al.* (1984)], consistent with prior cleavage of the 2′ C–N bond.

ESEEM spectroscopy of the N• generated during the incubation of the same [^2H]-labeled N_3UDPs with RDPR revealed interaction between the electron spin and the C-1′-^2H and C-4′-^2H nucleii (Figures 3 and 4). Both of these deuteriums are located, at least initially, on the α face of the nucleotide. No interactions with either the C-2′ or C-3′-^2Hs were observed (data not shown). The result with [3′-^2H]N_3-UDP is not surprising since its removal by a residue on the β face of N_3UDP is required to initiate the observed chemistry (Salowe *et al.*, 1987; Stubbe, 1989). However, the result with [2′-^2H]N_3UDP suggests that the 2-methylene-3(2*H*)-furanone is not yet generated and that C-2′ may be sp^3 hybridized with the [2′-^2H] on the β-face of the nucleotide. The interaction with C-1′-^2H suggests that the C-1′ carbon is also still sp^3 hybridized and the [1′-^2H] is on the α-face of the nucleotide. Otherwise, an interaction with the C-2′-^2H with N• might have been expected to be more likely than an interaction with C-1′-^2H. In harmony with this new proposal is the observation that the change in absorbance at 320 nm due to alkylation of RDPR by the furanone (Scheme II) occurs on a much slower time scale than the formation of the N• and loss of the Y•. The [5′-^3H]N_3UDP labeling experiments, which suggest that the transient nucleotide moiety (bound to R1 at the same time as the N•) is part of a reversible complex with R1/R2, are also consistent with this proposal. The EPR and ESEEM studies described above and the previous EPR studies in D_2O and with ^2H-labeled R2 (Sjöberg *et al.*, 1983; Ator *et al.*, 1984) leave few alternatives for the source of the proton which is coupled to N•. We propose that N• must be covalently bound to R1. Since C225 appears to be required for its generation and thiolates are known to reduce alkyl azides (Cartwright *et al.*, 1976; Stavos *et al.*, 1978), we propose that N• is covalently bound to cysteine 225. To account for the apparent 6.5 G doublet hyperfine interaction, the geometry of one of the β-hydrogens of the cysteine must be ~90° with respect to the orbital of the unpaired electron on the nitrogen such that its coupling constant is very small.

An alternative explanation for the putative doublet splitting must also be considered based on nitroxide spin labeling studies of Chignell et al. (1975) with egg white avidin. These workers observed that each of the three hyperfine lines due to the nitroxide were split into doublets, similar to the doublet we have attributed to hyperfine interaction with a proton. Since in their case no interactions with protons were feasible, they attributed this doublet splitting to dipole–dipole interactions between two spin labels bound to adjacent sites.[3] This explanation is probably not viable in the case of our N• for the following reasons. Although R2 is a homodimer, it contains at best 1.3 Y•s. The initial radical content is variable from preparation to preparation of R2, but the resulting EPR spectrum of the N• is always identical. In fact, the spectrum shown in Figure 2 was generated with R2 possessing onto 0.4 Y•s. In addition the R1 subunit, also a homodimer, loses only 50% of its activity, suggesting that only one of the two protomer

[3] We thank A. Gräslund for calling our attention to this paper.

sites per R1 is modified. Thus, it is unlikely that two N•s would ever be bound simultaneously to a 1:1 mixture of R1 and R2. The model we presently favor is that the doublet splitting of 6.5 G is due to hyperfine interaction with an adjacent proton derived from R1. Experiments are in progress to test this model.

Also unresolved is the large ^{14}N hyperfine interaction of 25 G. Such large splittings have only been observed in cases in which N is covalently bound to an oxygen. Incubation of N_3UDP and RDPR in the presence of $^{17}O_2$, however, has no effect on the spectrum of N• (data not shown).

Kinetics of Inactivation of RDPR by N_3UDP. To complement product identification studies on the interaction of N_3UDP with RDPR (Salowe *et al.*, 1987), the dynamics of this process have now been investigated. The models in Schemes I, II, and III predict that the Y• of R2 should be reduced concomitantly with 3′ C–H bond cleavage of N_3-UDP. To examine this prediction, the rates of loss of Y• were monitored upon incubation of RDPR with [3′-^{2}H]N_3UDP or [3′-^{1}H]N_3UDP. As indicated in Figure 6, the kinetics are, at a minimum, biphasic. An apparent isotope effect is observed on the rapid phase but not on the slower phase. Measurement of the initial rates of the fast phase as a function of the concentration of 3′-[^{1}H]- or [^{2}H]N_3UDP and analysis via the method of Cleland (1979) gave isotope effects on $^D(V)$ of 1.5 and $^D(V/K)$ of 2.2. These results are consistent with all of the models which require that cleavage of the 3′ C–H bond is coupled to loss of the Y•. The kinetics of the inactivation of RDPR were also examined with [^{1}H]- and [^{2}H]N_3UDPs. As indicated in Figure 7, an isotope effect is observed on this process as well. The kinetics are complex and are not amenable to an informative interpretation with the present level of mechanistic understanding.

The slow phase accompanying Y• loss is not understood. One can postulate, however, that the rate limiting step in this phase does not involve chemistry but perhaps involves subunit reorganization from an inactive conformation to an active conformation. There are at most 1.3 Y•s per R2, yet there are two putative substrate binding sites on R1. The fact that the specific activity of R1 is different from R2 when each subunit is assayed in the presence of an excess of the second subunit suggests that the one-to-one complex of R1/R2, proposed to be the active form of RDPR, needs to be reconsidered. To understand the slow phase of the reaction involving Y• loss, therefore, requires a better understanding of the dynamic interaction between the two subunits and whether the enzyme involves half sites reactivity.

Additional insight into the species responsible for the rapid and the slow inactivation processes was obtained by incubating [5′-^{3}H]N_3UDP with RDPR for various times and reisolating the protein by gel filtration under native and denaturing conditions. The observation that ^{3}H from [5′-^{3}H]N_3UDP is rapidly associated with the protein but may be released at short reaction times by denaturation indicates that the intermediate species is not covalently bound on the time scale of the enzyme inactivation. Therefore the chemistry proposed to occur in Scheme II leading to PP_i, uracil, and the reactive alkylating species appears to be relatively slow. On the other hand, the chemistry to convert the "azide" moiety to N_2 and N• appears to be on the same time scale as loss of the Y• (Sjöberg *et al.*, 1983; Ator *et al.*, 1984). Loss of the N• appears to be associated with PP_i, uracil, and furanone production and the covalent labeling of the protein. We postulate that the slow process, as described above, could involve dissociation of R2 from R1, facilitating access of the solvent to the active site of R1, leading to decomposition of the nucleotide intermediate and destruction of the N•. Efforts to trap this putative nucleotide intermediate by $NaBH_4$ reduction have thus far proven unsuccessful.

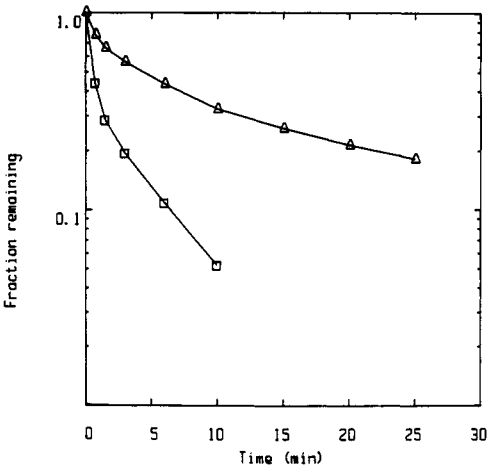

FIGURE 9: Time-dependent loss of activity and tyrosyl radical during reaction of N_3UDP with RDPR at 25 °C (△) tyrosyl radical loss and (□) CDP reduced.

The rapid loss of R1 specific activity (Figure 8) to less than 50% of the starting R1 activity provides further support for this model, if the quaternary complex of R1/R2/nucleotide/N• is catalytically inactive. The slower return of activity to approximately 50% may reflect dissociation of the inactive R2 and nucleotide fragments from R1, liberating the other active site of R1 for inhibitor turnover. In support of this thesis, addition of a second molar equivalent of R2 promoted additional turnover of N_3UDP during extended incubation times, destroying the additional Y• present and producing additional uracil in amounts proportional to the amount of R2 (data not shown).

Our previous studies defining the stoichiometry of product formation suggested that inactivation was governed by loss of Y• alone. If true, then Y• loss should occur at a rate greater than or equal to the rate of enzyme inactivation. The results presented in Figure 9 indicate that this is not the case.

An explanation for this observation is outlined in Scheme II and, as discussed subsequently, requires more than one turnover per inactivation event as well as multiple modes of inactivation. In the past few years, while investigating the interaction of site-directed mutants of R1 with CDP or the wild-type enzyme with a variety of new mechanism based inhibitors (Mao *et al.*, 1992a,b; Baker *et al.*, 1991), it has become clear that RDPR can be inactivated by multiple mechanisms. In Scheme II, the putative 3′-keto radical intermediate can be reduced by hydrogen atom transfer from a protein side chain on the top face or the bottom face of the nucleotide. Reduction from the top face (pathway a) regenerates the Y•. Inactivation would, therefore, result from alkylation of the enzyme by the 2-methylene-3-(2*H*)furanone and/or modification of an essential cysteine within the active site or a subsequent turnover involving pathway b (Scheme II). On the other hand, reduction from the bottom face of the nucleotide (pathway b, Scheme II) would result in irreversible loss of the Y• and, as a consequence, inactivation of the R2 subunit. In addition, furanone formation and/or active site cysteine modification could also lead to inactivation. Our initial studies of the inactivation of RDPR by N_3UDP in 1987 used R2 that had a specific activity of 3.3 μmol min^{-1} mg^{-1}. R2 used at present contains 1.3 Y•s per subunit and has a specific activity of 8.0–8.5 μmol min^{-1} mg^{-1}. Therefore,

it is possible that in our early experiments we were observing 1.5 turnovers relative to Y• prior to enzyme inactivation. This additional turnover and/or the multiple modes of inactivation would be sufficient to account for the observations made with both N_3UDP and N_3ADP (data not shown) that loss of the Y• is slower than inactivation. Thus, inactivation could result from loss of the Y•, modification of an active site cysteine, and/or alkylation by the furanone.

SUMMARY

Additional light has been shed on the mechanism of inactivation of RDPR by N_3UDP. Studies with 2′-[$^{15}N_3$,^{13}C]N_3UDP and with oxidized R1 and C225SR1 suggest that some form of N_3 is released prior to generation of N_2 and N•. These results are consistent with EPR studies using 1′-, 2′-, 3′-, or 4′-[^{2}H]N_3UDP, in which no alteration in the hyperfine interaction of the N• is observed. ESEEM studies, however, using these same compounds, reveal that the 1′ and 4′ deuterons are 3.3 ± 0.2 and 2.6 ± 0.3 Å, respectively, from the nitrogen-centered radical. The observation that the C225SR1 mutant and oxidized R1 fail to generate N• but that C462SR1 succeeds suggests that C225 is important in the conversion of the azide moiety to N_2 and N•.

Kinetic studies of the interaction of [3′-^{2}H]N_3UDP with RDPR indicate that there is an isotope effect on the loss of the Y• as well as on the inactivation process. Inactivation results from formation of a tight noncovalent complex which contains N• and (a) nucleotide intermediate(s). This complex collapses to form uracil, PPi, and 2-methylene-3(2*H*)-furanone. To account for the observation that Y• loss is slower than inactivation, multiple modes of inactivation, including alkylation by the furanone and/or modification of the active site cysteine, are required.

REFERENCES

Aberg, A., Hahne, S., Kurlsson, M., Larrson, A., Ormö, M., Ahgren, A., & Sjöberg, B. M. (1989) *J. Biol. Chem. 264*, 12249–12252.

Ames, B. N., & Dubin, D. T. (1960) *J. Biol. Chem. 235*, 769–775.

Atkin, C. L., Thelander, L., Reichard, P., & Lang, G. (1973) *J. Biol. Chem. 248*, 7464–7472.

Ator, M., Salowe, S. P., Stubbe, J., Emptage, M., & Robins, M. J. (1984) *J. Am. Chem. Soc. 106*, 1886–1887.

Baker, C. H., Banzon, J., Bollinger, J. M., Jr., Stubbe, J., Samano, V., Robins, M. J., Lippert, B., Jarvi, E., & Resvick, R. (1991) *J. Med. Chem. 34*, 1879–1884.

Britt, R. D., & Klein, M. P. (1987) *J. Magn. Reson. 74*, 535–540.

Cartwright, I. L., Hutchinson, D. W., & Armstrong, V. W. (1976) *Nucl. Acid Res. 3*, 2331–2339.

Chignell, C. F., Starkweather, D. K., & Sinah, B. K. (1975) *J. Biol. Chem. 250*, 5622–5629.

Cleland, W. W. (1979) *Methods Enzymol. 63*, 103–108.

Cook, A. F., & Moffat, J. G. (1967) *J. Am. Chem. Soc. 89*, 2697–2705.

Eriksson, S., Sjöberg, B.-M., Hahne, S., & Karlstrom, O. (1977) *J. Biol. Chem. 252*, 6132–6138.

Hampton, A., & Nichol, A. W. (1966) *Biochemistry 5*, 2076–2082.

Harris, G., Ator, M., & Stubbe, J. (1984) *Biochemistry 23*, 5214–5225.

Hobbs, J. B., & Eckstein, F. (1977) *J. Org. Chem. 42*, 714–719.

Kohn, P., Samarita, R. H., & Lerner, L. M. (1965) *J. Am. Chem. Soc. 87*, 5475–5480.

Kozarich, J. W., Chinault, A. C., & Hecht, S. M. (1973) *Biochemistry 12*, 4458–4463.

Krentitsky, T. A., Koszalka, G. W., & Tuttle, J. V. (1981) *Biochemistry 20*, 3615–3621.

Lunn, C. A., Kathju, S., Wallace, C., Kushner, S., & Pigiet, V. (1984) *J. Biol. Chem. 259*, 10469–10474.

Madhavan, C. V. B., & Martin, J. C. (1986) *J. Org. Chem. 51*, 1287–1293.

Magliozzo, R. S., McCracken, J., & Peisach, J. (1987) *Biochemistry 26*, 7923–7931.

Mao, S. S., Johnston, M. I., Bollinger, J. M. Jr., & Stubbe, J. (1989) *Proc. Natl. Acad. Sci. U.S.A. 86*, 1485–1490.

Mao, S. S., Holler, T. P., Yu, G.-X., Bollinger, J. M., Jr., Booker, S., Johnston, M. I., & Stubbe, J. (1992a) *Biochemistry 31*, 9733–9743.

Mao, S. S., Holler, T. P., Bollinger, J. M., Jr., Johnston, M. I., Yu, G. X., & Stubbe, J. (1992b) *Biochemistry 31*, 9744–9751.

McCracken, J., Peisach, J., & Dooley, D. W. (1987) *J. Am. Chem. Soc. 109*, 4064–4072.

Mims, W. B., & Peisach, J. (1989) in *Advanced EPR: Applications in Biology and Biochemistry* (Hoff, A. J., Ed.) pp 1–58, Elsevier, Amsterdam.

Mims, W. B., Davis, J. L., & Peisach, J. (1984) *Biophys. J. 45*, 755–766.

Moore, E. C., Reichard, P., & Thelander, L. (1964) *J. Biol. Chem. 239*, 3445–3452.

Nordlund, P., Sjöberg, B. M., & Eklund, H. (1990) *Nature 345*, 593–598.

Peisach, J., Mims, W. B., & Davis, J. L. (1979) *J. Biol. Chem. 254*, 12379–12389.

Penefsky, M. S. (1977) *J. Biol. Chem. 252*, 2891–2899.

Pigiet, V. P., & Conley, R. R. (1977) *J. Biol. Chem. 252*, 6367–6372.

Recondo, E. F., & Rinderknecht, H. (1959) *Helv. Chim. Acta 42*, 1171–1173.

Robins, M. J., Hawrelak, S. D., Hernandez, A. E., & Wnuk, S. F. (1992) *Nucleosides Nucleotides 11*, 821–834.

Russel, M., & Model, P. (1985) *J. Bacteriol. 163*, 238–242.

Salowe, S. P., & Stubbe, J. (1986) *J. Bacteriol. 165*, 363–366.

Salowe, S. P., Ator, M., & Stubbe, J. (1987) *Biochemistry 25*, 2256–2262.

Sjöberg, B.-M., Gräsland, A., & Eckstein, F. (1983) *J. Biol. Chem. 258*, 8060–8067.

Stavos, J. V., Bayley, H., Standring, D. N., & Knowles, J. R. (1978) *Biochem. Biophys. Res. Commun. 80*, 568–572.

Stubbe, J. (1989) *Adv. Enzymol. 63*, 349–420.

Stubbe, J. (1990) *J. Biol. Chem. 268*, 5329–5332.

Stubbe, J., & Ackles, D. (1980) *J. Biol. Chem. 255*, 8027–8030.

Thelander, L. (1973) *J. Biol. Chem. 248*, 4591–4601.

Thelander, L., & Reichard, P. (1979) *Annu. Rev. Biochem. 48*, 133–158.

Thelander, L., Larsson, B., Hobbs, J., & Eckstein, F. (1976) *J. Biol. Chem. 251*, 1398–1405.

Verheyden, J. P. H., Wagner, D., & Moffatt, J. G. (1971) *J. Org. Chem. 36*, 250–254.

Vorbrüggen, H., & Bennua, B. (1981) *Chem. Ber. 114*, 1279–1286.

Vorbrüggen, H., Krolikiewicz, K., & Bennua, B. (1981) *Chem. Ber. 114*, 1234–1255.

Yoshikawa, M., Kato, T., & Takenishi, T. (1967) *Tetrahedron Lett.* 5065–5068.